

BACKGROUND

- Sharpness-Aware Minimization (SAM)** directs the search for model parameters within flat regions by minimizing the maximum loss in the vicinity of weight \mathbf{w} within a radius ρ

$$\min_{\mathbf{w}} L^{\text{SAM}}(\mathbf{w}) \text{ where } L^{\text{SAM}}(\mathbf{w}) = \max_{\|\mathbf{v}\|_2 \leq 1} L_S(\mathbf{w} + \rho\mathbf{v})$$

- SAM employs one-step gradient ascent to approximate the inner maximization

$$\nabla L^{\text{SAM}}(\mathbf{w}) \approx \nabla L_S \left(\mathbf{w} + \rho \frac{\nabla L_S(\mathbf{w})}{\|\nabla L_S(\mathbf{w})\|_2} \right)$$

PITFALLS IDENTIFIED (by us)

- Deterioration of one-step sharpness approximation as training proceeds.**

We define *approximation ratio* (AR):

$$\text{AR} = \mathbb{E}_{(x,y) \sim D} \left[\frac{\ell(f(x; \mathbf{w} + \delta), y) - \ell(f(x; \mathbf{w}), y)}{\ell(f(x; \mathbf{w} + \delta^*), y) - \ell(f(x; \mathbf{w}), y)} \right]$$

where δ represents *one-step* gradient ascent perturbation, and δ^* denotes the optimal perturbation which is calculated with 20-step gradient ascent.

- Conventional Hessian fails to capture true loss landscape curvature**

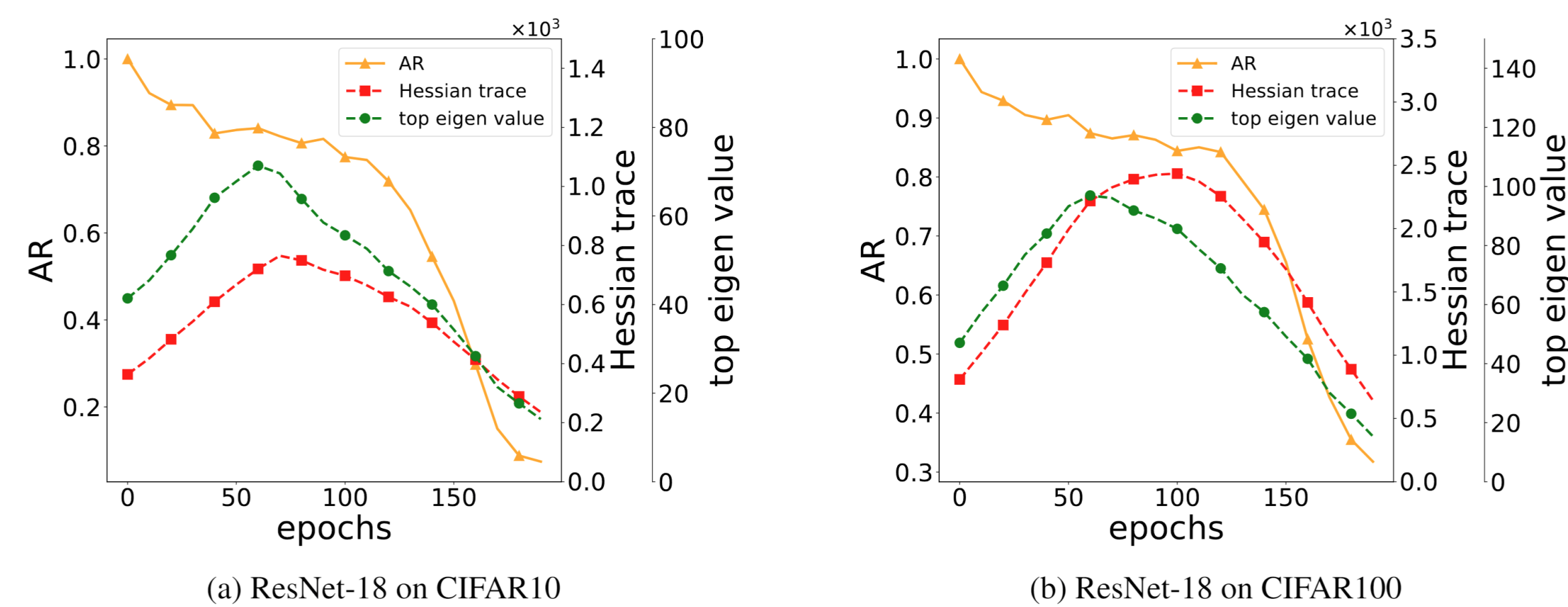


Figure 1. Evolution of approximation ratio (AR), Hessian trace, and top eigenvalue of Hessian during SAM training on CIFAR10 and CIFAR100 datasets. The continuously **decreasing AR** indicates an **enlarging curvature** whereas **both of the Hessian-based curvature metrics**, Hessian trace and the top eigenvalue (which are expected to continuously increase) **fail to capture** the true curvature of model loss landscape.

RESOURCES AND CONTACT

- Paper:** <https://arxiv.org/abs/2312.13555>
- Code:** <https://github.com/TrustAloT/CR-SAM>
- Contact:** wuta@mst.edu, tluo@mst.edu, dwunsch@mst.edu

METHODS

- Propose a new metric for accurate curvature characterization, called *normalized Hessian trace*:**

$$\mathcal{C}(\mathbf{w}) = \frac{\text{Tr}(\nabla^2 L_S(\mathbf{w}))}{\|\nabla L_S(\mathbf{w})\|_2}$$

- Characterizes curvature faithfully**
- Consistent trends on both training and test sets**

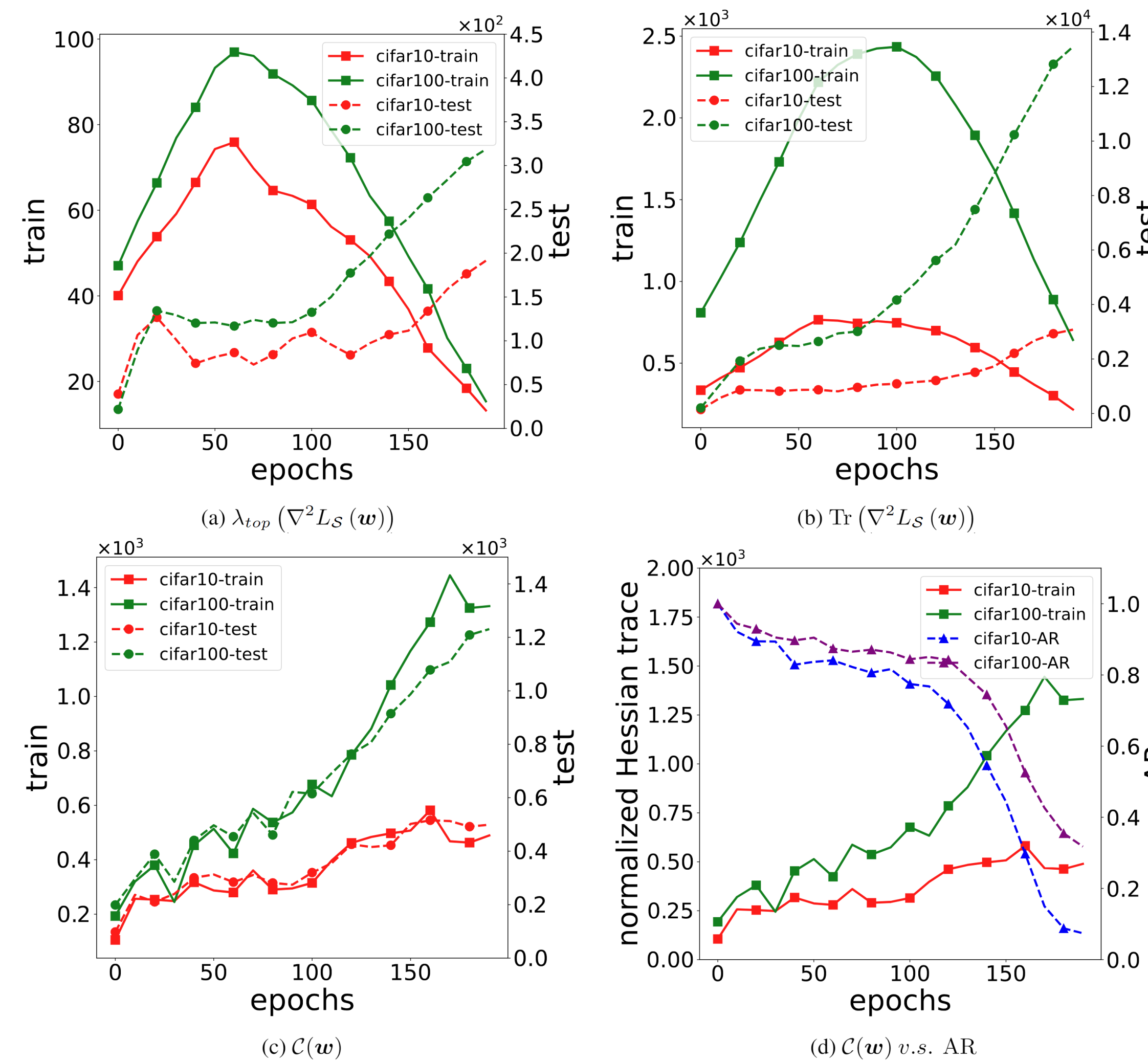


Figure 2. The **normalized Hessian trace (d)** indicates a **growing curvature** throughout training which explains the phenomenon of **decreasing AR** (approximation ratio). In addition, it behaves **consistently** on both train and test sets (c; as opposed to a & b which are conventional Hessian).

- Curvature Regularized Sharpness-Aware Minimization (CR-SAM)**

$$R_c(\mathbf{w}) = \alpha \log \text{Tr}(\nabla^2 L_S(\mathbf{w})) + \beta \log \|\nabla L_S(\mathbf{w})\|_2$$

$$\min_{\mathbf{w}} L^{\text{CR-SAM}}(\mathbf{w})$$

$$\text{where } L^{\text{CR-SAM}}(\mathbf{w}) = L^{\text{SAM}}(\mathbf{w}) + R_c(\mathbf{w})$$

Solving it with *finite difference method*:

$$R_c(\mathbf{w}) = \mathbb{E}_{\mathbf{v} \sim N(0, I)} \left[\alpha \log (L_S(\mathbf{w} + \rho\mathbf{v}) + L_S(\mathbf{w} - \rho\mathbf{v}) - 2L_S(\mathbf{w})) + \beta \log (L_S(\mathbf{w} + \rho\mathbf{v}) - L_S(\mathbf{w} - \rho\mathbf{v})) \right]$$

RESULTS

Model	Aug	CIFAR-10			CIFAR-100		
		SGD	SAM	CR-SAM	SGD	SAM	CR-SAM
ResNet-18	Basic	95.29 \pm 0.16	96.46 \pm 0.18	96.95 \pm 0.13	78.34 \pm 0.22	79.81 \pm 0.18	80.76 \pm 0.21
	Cutout	95.96 \pm 0.13	96.55 \pm 0.15	97.01 \pm 0.21	79.23 \pm 0.13	80.15 \pm 0.17	81.26 \pm 0.19
	AA	96.33 \pm 0.15	96.75 \pm 0.18	97.27 \pm 0.12	79.05 \pm 0.17	81.26 \pm 0.21	82.11 \pm 0.22
ResNet-101	Basic	96.35 \pm 0.12	96.51 \pm 0.16	97.14 \pm 0.11	80.54 \pm 0.13	82.11 \pm 0.12	83.03 \pm 0.17
	Cutout	96.56 \pm 0.18	96.95 \pm 0.13	97.51 \pm 0.24	81.26 \pm 0.21	82.39 \pm 0.27	83.46 \pm 0.16
	AA	96.78 \pm 0.14	97.11 \pm 0.16	97.76 \pm 0.16	81.83 \pm 0.37	83.25 \pm 0.47	84.19 \pm 0.23
WRN-28-10	Basic	95.89 \pm 0.21	96.81 \pm 0.26	97.36 \pm 0.15	81.84 \pm 0.13	83.15 \pm 0.14	84.45 \pm 0.09
	Cutout	96.89 \pm 0.07	97.55 \pm 0.16	97.98 \pm 0.21	81.96 \pm 0.40	83.47 \pm 0.15	84.48 \pm 0.13
	AA	96.93 \pm 0.12	97.59 \pm 0.06	97.94 \pm 0.08	82.16 \pm 0.11	83.69 \pm 0.26	84.74 \pm 0.21
PyramidNet-110	Basic	96.27 \pm 0.13	97.34 \pm 0.13	97.89 \pm 0.08	83.27 \pm 0.12	84.89 \pm 0.09	85.68 \pm 0.14
	Cutout	96.79 \pm 0.13	97.61 \pm 0.21	98.08 \pm 0.11	83.43 \pm 0.21	84.97 \pm 0.17	85.86 \pm 0.21
	AA	96.97 \pm 0.08	97.81 \pm 0.13	98.26 \pm 0.11	84.59 \pm 0.08	85.76 \pm 0.23	86.58 \pm 0.14

Table 1. Classification accuracy on CIFAR-10 and CIFAR-100 datasets.

Optimizer	$\ \nabla L_S(\mathbf{w})\ _2$	$\text{Tr}(\nabla^2 L_S(\mathbf{w}))$	$\mathcal{C}(\mathbf{w})$
SGD	19.97 \pm 0.52	32673 \pm 1497	1674 \pm 78
SAM	11.51 \pm 0.31	14176 \pm 327	1193 \pm 59
CR-SAM	8.26 \pm 0.19	7968 \pm 145	884 \pm 23

Table 2. Model geometry (characterized by 3 metrics) of ResNet-18 trained with SGD, SAM and CR-SAM. Values are computed on test set. It shows the CR-SAM optimizer achieves the minimal in all cases.

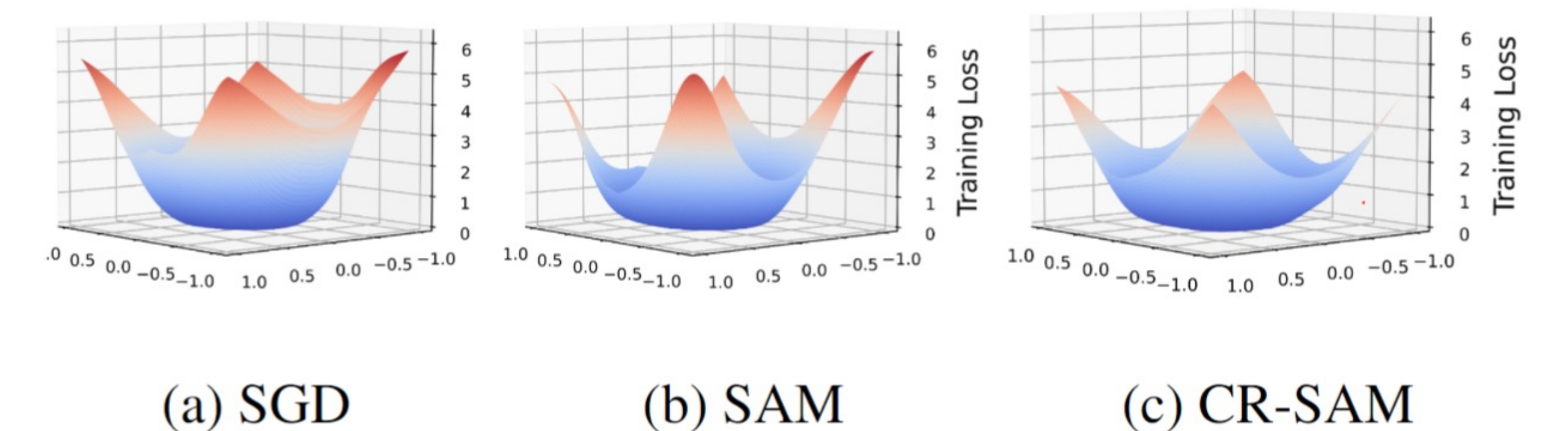


Figure 3. CR-SAM yields flatter loss landscape.

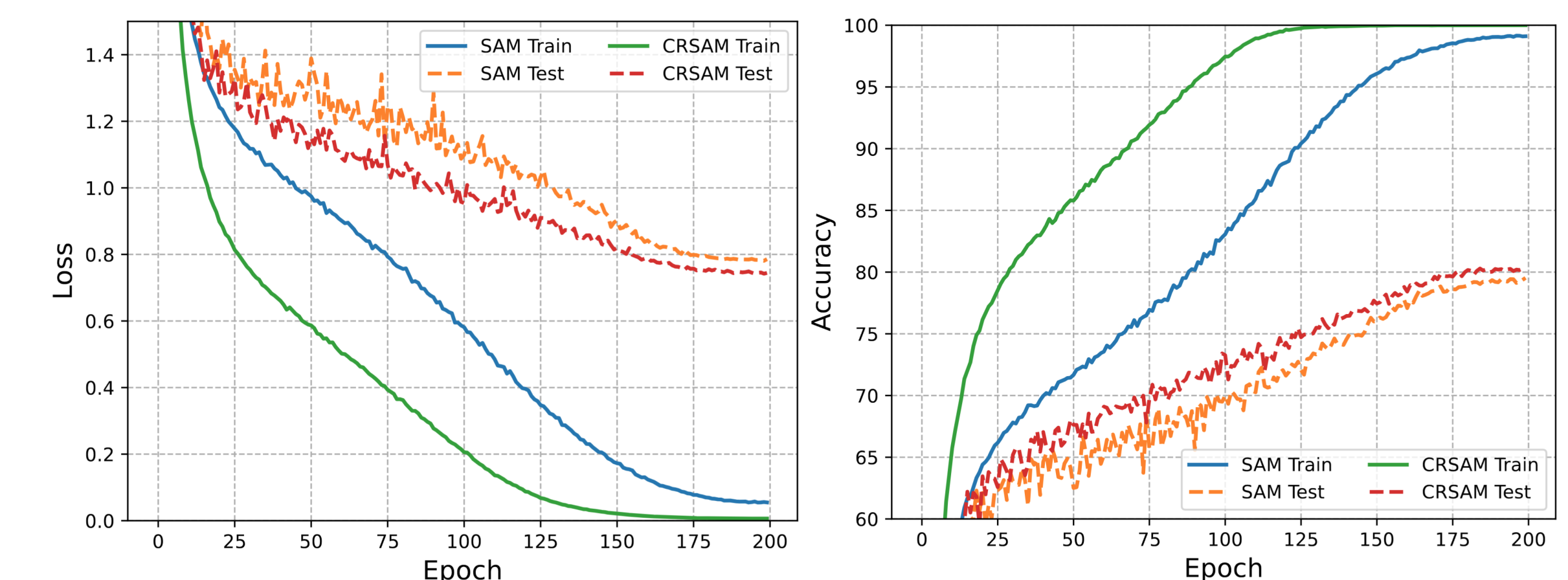


Figure 4. CR-SAM achieves **much faster and stabler convergence**. This can be explained by the fact that **CR-SAM discourages excessive curvature** and thus reduces optimization complexity, making local minima easier to reach.